Solitons and Precision Neutrino Mass Spectroscopy

M. Yoshimura
Center of Quantum Universe, Faculty of Science, Okayama University
Tsushima-naka 3-1-1 Kita-ku Okayama 700-8530 Japan

ABSTRACT

We propose how to implement precision neutrino mass spectroscopy using radiative neutrino pair emission (RNPE) from a macro-coherent decay of a new form of target state, a large number of activated atoms interacting with static condensate field. This method makes it possible to measure still undetermined parameters of the neutrino mass matrix, two CP violating Majorana phases, the unknown mixing angle and the smallest neutrino mass which could be of order a few meV, determining at the same time the Majorana or Dirac nature of masses. The twin process of paired superradiance (PSR) is also discussed.

Introduction Neutrinos are still mysterious particles: their absolute mass scale (or the smallest neutrino mass), the nature of masses (whether they have Majorana or Dirac type masses), and their relation to the leptogenesis theory [1], [2] are not clarified experimentally. Experimental efforts to unravel these properties are mainly focused on nuclear targets. Nuclear targets, however, are problematic at least in one important aspect, the mismatch of energy scale: the released energy of nuclear transition is of order several MeV, and this is far separated from the expected neutrino mass range of O[0.1]eV.

We proposed a few years ago the idea of using atomic targets to overcome this difficulty; RNPE from a metastable state $|e\rangle$, $|e\rangle \rightarrow |g\rangle + \gamma + \nu_i\nu_j$. This is an elementary process predicted by the ordinary electroweak interaction, and its detection opens a path towards the neutrino mass spectroscopy [3], [4], by precisely measuring the photon energy spectrum, thereby resolving neutrino mass eigenstates $\nu_i\,, i = 1, 2, 3$.

With smaller released energies of atomic transitions, the atomic decay involving neutrino pair emission has a demerit of tiny weak rates, unless a new idea of rate enhancement is taken into account. Our enhancement mechanism uses a coherent cooperative effect of a large number of atoms interacting with a common field [5], [6]. A similar idea goes back to the superradiance (SR for short) [7] of a single photon emission, where the decay rate from many atoms is in proportion to n^2V, the target number density squared times a coherent volume V, unlike the target number nV in the spontaneous decay.

Atoms in a metastable state $|e\rangle$ may have a lifetime for a long time measurement. If these atoms further have a developed coherence, macro-coherent two photon emission, called paired superradiance (PSR for short), $|e\rangle \rightarrow |g\rangle + \gamma + \gamma$, becomes easily detectable [5], its rate $\propto n^2V$, with V a macroscopic target volume, unlike the case of usual SR limited by $V \propto$ the photon wavelength squared. PSR has a distinct signature: two photons are back to back emitted and have exactly the same energy.

We propose in this work to use for the target of RNPE a coherent state of atoms interacting with static field condensate (we call this as condensate for simplicity). The condensate is a limiting case of multiple soliton solutions, as presented below. Both solitons and condensate are proved stable against PSR, but unstable for RNPE.

PSR, emitting a highly correlated pair of two photons, is interesting from points of application such as quantum entanglement. Artificial destruction of solitons and condensate, which can be easily realized by a sudden application of electric pulse (thus abruptly changing the dielectric constant), provides the most efficient mechanism of PSR emission yet to be discovered. If we successfully destroy solitons for PSR under complete control, solitons may become qubits for quantum computing.

On the other hand, creation and subsequent long time control of the condensate removes the most serious PSR background for RNPE. We compute macro-coherent RNPE rate $\propto n^2V$ of condensate decay and study sensitivity of spectral rates (spectral shape and event rate) to parameters of the neutrino mass matrix, most importantly the fundamental parameter of CP violating Majorana phases; the parameter of central importance in explaining the matter-antimatter imbalance of the universe. RNPE spectrum shape from the condensate decay is time independent after condensate formation and the most unambiguous tool for this process.

Our method uses laser to trigger RNPE at non-resonant frequencies, which should be a great merit since the trigger is not destructive to target atoms.

The natural unit $\hbar = c = 1$ is used in formulas of this paper.

Effective atomic Hamiltonian and Maxwell-Bloch equation We consider atoms that consist of three levels of energies $\epsilon_g < \epsilon_e < \epsilon_p$. The state $|e\rangle$, for example $^1D_2$-state of Ba low lying levels, is forbidden to decay to $|g\rangle$ by E1 transition, while E1 transitions from $|p\rangle$ to $|e\rangle$ and $|g\rangle$ may both be allowed. The important part of Hamiltonian is derived [8], [6] by eliminating time memory

effects of $|p\rangle$, ${}^1P_1$ in Ba, and by making a slowly varying envelope approximation of one field mode propagating in a direction. The resulting effective Hamiltonian is restricted to two levels, $|e\rangle$ and $|g\rangle$, interacting with field E of frequency ω and a definite polarization. The 2×2 matrix elements $\mu_{ab}\,, a, b = e, g$, are Stark energies; a product of two dipole (E1 or M1) transition elements to $|p\rangle$ times the electric field squared. Dipole transition elements are related to measurable decay rates $\gamma_{pa}\,, a = e, g$ from $|p\rangle$ to $|a\rangle$, thus

$$\mu_{aa} = \frac{6\pi\gamma_{pa}}{\epsilon_{pa}^2(\epsilon_{pa}^2-\omega^2)}\,, \qquad (a = e\,, g)\,, \tag{1}$$

$$\mu_{eg} = \mu_{ge} = \frac{3\pi(\epsilon_{pe}+\epsilon_{pg})}{2(\epsilon_{pe}-\omega)(\epsilon_{pg}+\omega)}\sqrt{\frac{\gamma_{pe}\gamma_{pg}}{\epsilon_{pe}^3\epsilon_{pg}^3}}\,. \tag{2}$$

We ignored the spin multiplicity factor $2J_a+1$ in the relation d_{ab}^2 to γ_{ab}. The final PSR rate formula should be multiplied by $(2J_p+1)/(2J_e+1)$ if one includes this multiplicity.

The equation for the polarization vector $\vec{R}$ (3 bilinears of amplitudes times the target number density n), called the Bloch equation, is derived from the Schrödinger equation, and may be written as $\partial_t\vec{R} = |E|^2\mathcal{M}\vec{R}\,,$ where elements of 3×3 anti-symmetric matrix $\mathcal{M}$ are linear combinations of μ_{ab}. When this equation is combined with the Maxwell equation, written as $(\partial_t+\partial_x)|E|^2 = \omega\mu_{ge}|E|^2R\,,$ with R a component of $\vec{R}$, a closed set of equations follows, to describe spacetime evolution of polarization and propagating field [8], [6].

When relaxation processes are ignored, one can introduce the tipping angle $\theta(x,t)$ by $R(x,t) = n\cos\theta(x,t)$. The Bloch equation is then reduced to a relation of $\theta(x,t)$ to the electric field strength; $|E(x,t)|^2 = \partial_t\theta/\mu$ with $\mu = \sqrt{(\mu_{ee}-\mu_{gg})^2+4\mu_{ge}^2}/4$. The field $\theta(x,t)$ is an analogue of the area for field propagation in the two-level problem [9]. The Maxwell equation in terms of $\theta(x,t)$ is

$$(\partial_t+\partial_x)\theta = \alpha_m(-\cos\theta + A)\,, \tag{3}$$

$$\alpha_m = 6\pi\sqrt{\frac{\gamma_{pe}\gamma_{pg}}{\epsilon_{pe}^3\epsilon_{pg}^3}}\frac{\omega n}{\epsilon_{pe}+\epsilon_{pg}}\,, \tag{4}$$

where $\epsilon_{ba} = \epsilon_b - \epsilon_a$ is the atomic energy difference. For the Ba D-state, $\alpha_m \sim 2.4\times 10^{-6}\mathrm{cm}^{-1}(n/10^{12}\mathrm{cm}^{-3})$ at $\omega = \epsilon_{eg}/2$. Both α_m and μ depend on ω. The non-linear equation (3) describes dynamics of a fictitious pendulum under friction periodically varying $\propto \alpha_m\sin\theta$ at its location θ.

For $|A|\le 1$, the tipping angle is restricted to a finite $\theta-$region of $\le 2\pi$. The propagation problem in this case has been analytically solved in [6] in terms of arbitrary initial data. Hence the system appears integrable in the mathematical sense. Typical solutions describe multiple splitting of pulses and their compression when they propagate in a long coherent medium, as fully explained in [6]. The number of split pulses is given by the initial pulse area $\theta(-\infty,\infty)$ divided by 2π. This behavior of pulse in medium is a symptom of instability, and pulses stabilize via PSR. It is thus anticipated that stable objects against PSR exist; solitons.

Soliton solutions There are two types of analytic solutions for solitons; $|A| = 1$ giving a single soliton of quantized area 2π and $|A| > 1$ the multiple soliton. The case $|A| < 1$ is unphysical since an excited state of population $n\cos\theta \ne -n$ exists at $\xi = \pm\infty$. The case of $|A| = 1$ solution of area 2π has been obtained in [6] by using a different method.

We look for soliton solutions by assuming one variable dependence of $x-vt$ for a soliton of velocity v and by reducing the partial differential equation to an ordinary one. The solution for $A = 1$ thus

obtained has a Lorentzian shape of flux and the population given by

$$|E_s(x,t)|^2 = \frac{2\alpha_m}{\mu}\frac{v(1-v)}{\alpha_m^2(x-vt)^2+(1-v)^2}\,, \tag{5}$$

$$\cos\theta_s(x,t) = \frac{-\alpha_m^2(x-vt)^2+(1-v)^2}{\alpha_m^2(x-vt)^2+(1-v)^2}\,. \tag{6}$$

The soliton size is $O[1/\alpha_m]$, and its field flux is of order, $\alpha_m/\mu \sim 30\mathrm{Wmm}^{-2}(n/10^{18}\mathrm{cm}^{-3})$ for the Ba soliton at $\omega = \epsilon_{eg}/2$.

This method applied to the $|A| > 1$ case, on the other hand, gives a new class of solutions given by

$$|E(x,t)|^2 = \frac{\alpha_m}{\mu}\frac{v}{1-v}\frac{A^2-1}{A-\cos X}\,, \quad \cos\theta(x,t) = \frac{A\cos X - 1}{A-\cos X}\,, \tag{7}$$

$$X = \frac{\alpha_m\sqrt{A^2-1}}{1-v}(x-vt)\,. \tag{8}$$

Unlike the single peak for $|A| = 1$, the field flux given by (7) has infinitely many peaks equally spaced, describing multiple soliton solutions in medium.

For a finite length of medium one may impose the boundary condition of no excited state at two target ends of $x = \pm L/2$. This gives a condition, $\alpha_m L\sqrt{A^2-1}/(1-v) = 2\pi(2n_s-1)\,, n_s = 1, 2, \cdots$. The quantity $\sqrt{A^2-1}$ is of order, and the soliton number density $\sim n_s/(\alpha_m L)$.

Solitons may both emit and absorb photons within medium, their rate difference $\propto \cos\theta|E(x,t)|^2$. This quantity, when integrated in the entire medium supporting a soliton, gives an integral of a total derivative $\propto \partial_x \sin\theta$, hence vanishes for the quantized area of $\Delta\theta = 2\pi$. This proves the soliton stability against PSR.

Field condensate One may consider the limit of large soliton density, $n_s/\alpha_m L \sim \sqrt{A^2-1}/4\pi \to \infty$, simultaneous with the limit $v \to 0$. Denoting $A = \sqrt{(\eta/v)^2+1}$ with η kept constant, one has

$$|E_c(x.t)|^2 = \frac{\alpha_m\eta^2}{\mu\,(\eta - v\cos(\alpha_m\eta(x-vt)/v))} \approx \frac{\eta\alpha_m}{\mu}\,, \tag{9}$$

thus an almost constant field flux is derived. The population $\propto \cos\theta$ oscillates, with the time period $\tau = 2\pi/(\alpha_m\eta)$ and the space period τv. The parameter η is $4\pi\times$ soliton density $\times$ soliton velocity.

Practically, the shortest spatial period is limited by the inter-atomic distance d. By identifying the period τv with d, one finds $\eta \sim 2\pi v/(\alpha_m d)$, hence $\tau = d/v$. As $v \to 0$, $\tau \to \infty$, and the target becomes fully excited with $\cos\theta = 1$. For the Ba $^1\mathrm{D}_2$-state, the relevant numerical value is $\alpha_m d \sim 4\times 10^{-7}(n/10^{18}\mathrm{cm}^{-3})^{2/3}$.

The limit taken here gives a constant field $\eta\alpha_m/\mu$ and the full excitation of target everywhere (strictly, this is true for an infinitely long medium). This is the state of field condensate we use for RNPE. Field condensate can be created by trigger laser irradiation from multiple directions, since it has no memory of a particular direction.

The stability analysis around the condensate can be made, taking $E = E_c + \delta E\,, \theta = \theta_c + \delta\theta$ with $E_c\,, \theta_c = 0$ the condensate solution. By keeping linear terms $\propto \delta E, \delta\theta$ in the Maxwell-Bloch equation, with $\delta E, \delta\theta \propto e^{-i\omega t}$ for time dependence, the perturbation equation $\partial_x\delta E = i(\omega + \alpha_m^2\eta/\omega)\delta E$ gives a bounded and purely oscillatory solution, indicating the stability of field condensate.

PSR rate at soliton and condensate destruction We first mention PSR rate without soliton creation. The PSR rate without trigger is $\mu_{ge}^2\epsilon_{eg}^4 n^2 V/(2^9\pi^2)$, which is numerically $\sim$

$0.5\text{MHz}(n/10^{12}\text{cm}^{-3})^2 V/\text{cm}^3$ for Ba. Under a strong trigger of flux $|E|^2$, the rate for a target of length L becomes [6]

$$\frac{\mu_{ge}^2 \epsilon_{eg} n^2 V L |E|^2}{32\pi} \,. \tag{10}$$

Although the rate for $|E|^2 \approx 10^6 \text{Wcm}^{-2}$ is large, time structure of PSR is complicated [6].

PSR after soliton formation occurs only at its destruction, without absorption from $|g\rangle$. The emission rate from $|e\rangle$ is $\propto (1+\cos\theta)|E_s|^2/2$. One may compute rates based on perturbative methods, in which one of the photons belongs to the soliton pulse. The other photon is emitted backward to the soliton propagation direction, with exactly the same energy. The large rate enhancement $\propto n^2 V$ is understood by the momentum conservation among emitted particles, implying $e^{i(\vec{k}+\vec{k'})\cdot\vec{x}} = 1$.

The PSR rate at soliton destruction is (taking $L = dx$ in eq. (10))

$$d\Gamma(x,t) = \frac{\mu_{ge}^2 \alpha_m \epsilon_{eg} n^2 V}{16\pi\mu} \frac{v(1-v)}{\alpha_m^2 (x-vt)^2 + (1-v)^2} dx \,. \tag{11}$$

The rate remains large during a time of

$$\Delta t = \frac{1-v}{v\alpha_m} \sim 14\mu\text{sec} \frac{1-v}{v} \frac{10^{12}\text{cm}^{-3}}{n} \,. \tag{12}$$

The space integrated rate per soliton is

$$\frac{\mu_{ge}^2 \epsilon_{eg} v n^2 V}{16\mu} \sim 5 \times 10^{15}\text{Hz} \frac{v n^2 V}{10^{24}\text{cm}^{-3}} \,, \tag{13}$$

(numbers for Ba) a formula valid for a target of length $L \gg 1/\alpha_m$. For a short target of $L \leq 1/\alpha_m$ the rate is reduced by $\alpha_m L/(\pi(1-v))$. The integrated rate for long target is by many orders ($\sim 10^8$) larger than the trigger-less PSR rate. The prolonged time of $O[1]\mu$sec and its simple profile structure has a number of merits of easier PSR identification such as the back to back two photon coincidence measurement. PSR rate at condensate destruction is larger by $\eta\alpha_m L/(v\pi)$ than at the single soliton destruction.

Effect of relaxation There are a number of processes that might destroy coherence. One of them is given by a field decay, introduced by a term $\kappa|E|^2$ in the Maxwell equation. This modifies the basic equation (3) by an additional term $-\kappa\theta$. With the ansatz of variable dependence of $\xi = x - vt$, this equation is

$$(1-v)\frac{d\theta}{d\xi} = -\alpha_m \cos\theta - \kappa\theta \,. \tag{14}$$

Direct numerical integration of eq.(14) gives distorted quasi-soliton solutions. Their profile, although distorted, is unchanged as they propagate. Quasi-solitons exist only for $\kappa < \kappa_c$ where $\kappa_c \sim 0.725\alpha_m$, indicating a threshold of dissipation. Calculation gives the PSR rate = (PSR rate at pure soliton destruction) $\times \Delta(\theta + \sin\theta)/2\pi$ (the difference Δ to be taken at two target ends). This rate is smaller than the one without dissipation, but not very much less, unless κ is very close to the threshold κ_c. The condition of a sizable PSR rate, the relaxation constant $\kappa < O[\alpha_m]$, implies that $\kappa < O[0.07]\text{MHz}(n/10^{12}\text{cm}^{-3})$ for the Ba target.

RNPE The effective Hamiltonian for RNPE,

$$\frac{G_F \vec{S}_e \cdot \sum_{ij} c_{ij} \nu_j^\dagger \vec{\sigma} \nu_i}{\epsilon_{pg} - \omega} \vec{d} \cdot \vec{E} \,, \tag{15}$$

gives the amplitude for a single atom, where $\vec{S}_e$ and $\vec{d}$ are electronic spin and dipole operators. To give large matrix elements for these, we consider deexcitation of $|e\rangle$ of the angular momentum $J = 2$ or $J = 0$ to $|g\rangle$ of $J = 0$ via $|p\rangle$ of $J = 1$, realized by rare gas and alkhali earth atoms. Six measurable constants, c_{ij}'s, given by $c_{ij} = U^*_{ei}U_{ej} - \delta_{ij}/2$ with U the unitary matrix relating the neutrino flavor to the mass eigenstate, contain mixing angles and Majorana CP phases [3], [4].

The field operator ν_i for the Majorana neutrino is a superposition of annihilation (b_i) and creation ($b_i^\dagger$) operator of the same Majorana particle, while for the Dirac neutrino it is a sum of two distinct operators; particle annihilation (b_i) and anti-particle creation ($d_i^\dagger$). Thus, the $\nu_i\nu_j$ pair emission amplitude for $i \neq j$ has the form, $b_i^\dagger b_j^\dagger(c_{ij} - c_{ji})/\sqrt{2} = i\sqrt{2}\Im c_{ij} b_i^\dagger b_j^\dagger$ for the Majorana case, and $c_{ij} b_i^\dagger d_j^\dagger$ for the Dirac case. Condensate RNPE decay rate of field $|E_c|^2 \sim \eta\alpha_m/\mu$ is a sum of 6 $\nu_i\nu_j$ pair emission;

$$\frac{48n^2V\eta\alpha_m G_F^2\gamma_{pg}}{\epsilon_{pg}^3(\epsilon_{pg}-\omega)^2\mu}\sum_{ij} B_{ij}I_{ij}(\omega)\,. \tag{16}$$

For $i \neq j$, $B_{ij} = (\Im c_{ij})^2$ for the Majorana case and $B_{ij} = |c_{ij}|^2$ for the Dirac case, while $B_{ii} = |c_{ii}|^2$ for both cases. Factors, α_m and μ, attributed to condensate parameters, involve intermediate $|p\rangle$. The state $|p\rangle$ that gives the largest condensate factor may be different from the intermediate state that gives the largest RNPE rate. In the Yb case, $|p\rangle = 6s6p^3P_1$ for the largest condensate factor and $|p\rangle = 6s6p^1P_1$ for the largest RNPE rate.

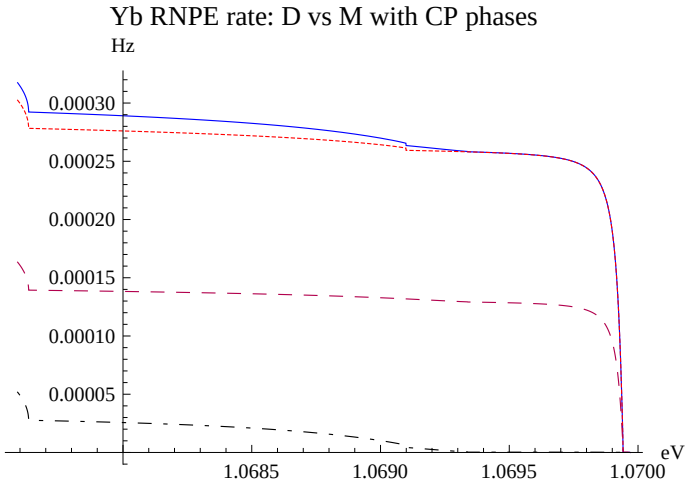

Figure 1: Yb RNPE photon energy spectrum in (11) $\sim$ (33) region from condensate decay. Dirac case and 3 Majorana cases of different (α, β) are plotted; Dirac in blue, $(\pi/2, 0)$ Majorana in dotted or short dashed red, $(0, \pi/2)$ Majorana in broken black, and $(\pi/4, -\pi/4)$ Majorana in dashed purple. Neutrino masses of $(m_1, m_2, m_3) = (50, 10, 1)$meV, and cosine angles $1/\sqrt{2}, \sqrt{3}/2, \sqrt{0.97}$ are assumed for all. The Majorana pair emission rate of (α, β) = (0,0) below (3,3) neutrino threshold is by $\sim 10^{-3}$ smaller than the Dirac rate for these masses. Assumed target parameters are $n = 10^{21}\text{cm}^{-3}$, $V = 1\text{cm}^3$, and $\eta = 10^3$.

The function $I_{ij}(\omega)$ in the formula (16) is given by an energy integral arising from the two neutrino

phase space. The integral in a symmetric form is given in terms of neutrino energies $E_i\,, i=1,2$,

$$I_{ij}(\omega)=\omega\int_0^\infty\int_0^\infty dE_1dE_2\delta(E_1+E_2+\omega-\epsilon_{eg})\theta(C_{ij}(E_1,E_2))\left(\frac{K_{ij}^{(1)}}{12}+\frac{3K_{ij}^{(2)}}{4}\right), \quad (17)$$

$$K_{ij}^{(1)}=2G_{ij}^{(1)}(E_1,E_2)\,,\ K_{ij}^{(2)}=-G_{ij}^{(1)}(E_1,E_2)+G_{ij}^{(2)}(E_1,E_2)+\frac{E_1E_2-\delta_M m_im_j}{\omega^2}\,, \quad (18)$$

$$G_{ij}^{(1)}=\frac{1}{8}+\frac{E_1^2+E_2^2-m_i^2-m_j^2}{4\omega^2}-3\frac{(E_1^2-E_2^2-m_i^2+m_j^2)^2}{8\omega^4}\,, \quad (19)$$

$$G_{ij}^{(2)}=\frac{1}{8}-\frac{E_1^2+E_2^2-m_i^2-m_j^2}{4\omega^2}+\frac{(E_1^2-E_2^2-m_i^2+m_j^2)^2}{8\omega^4}\,, \quad (20)$$

where the boundary region is given by $C_{ij}(E_1,E_2)\geq 0$ with

$$C_{ij}(E_1,E_2)=(E_1^2+E_2^2-m_i^2-m_j^2-\omega^2)^2-4(E_1^2-m_i^2)(E_2^2-m_j^2)\,, \quad (21)$$

and $\delta_M=1$ for the Majorana and $\delta_M=0$ for the Dirac case. In this calculation, averaged electron spin matrix elements, $\langle(\vec{k}\cdot\vec{S}_e/\omega)^2\rangle=1/12\,,\langle\vec{S}_e^2\rangle=3/4$, are used. The resulting spectrum given by (16) sharply rises at each (ij) threshold, a feature characteristic of 3 particle emission of massless γ and nearly massless ν_i,ν_j, when both the momentum and the energy conservation hold.

The limiting case of 3 massless neutrinos gives RNPE rate of the condensate decay,

$$\frac{G_F^2\gamma_{pg}\epsilon_{eg}^2n^2V\eta\alpha_m}{\mu\epsilon_{pg}^5}f(\frac{2\omega}{\epsilon_{eg}})\,,\quad f(x)=\frac{9(324-540x+245x^2)}{32(1-\epsilon_{eg}x/(2\epsilon_{pg}))^2}\,. \quad (22)$$

The coefficient in front of the function $f(2\omega/\epsilon_{eg})$ is not rapidly varying with the photon energy ω in the neutrino threshold regions, and on the average over the photon energy to 0.95eV, $\sim 8\times10^{-5}$Hz for Yb of $n=10^{21}\mathrm{cm}^{-3}\,,V=1\mathrm{cm}3\,,\eta=10^3$.

Experiments for the neutrino spectroscopy are to be performed keeping the macro-coherence of the condensate. The initial trigger frequency $\omega\leq\omega_{11}$ for RNPE of $\omega_{11}=\epsilon_{eg}/2-2m_1^2/\epsilon_{eg}$, with m_1 the smallest neutrino mass, is reset each time for measurements of rate and parity violating quantities [4] at different γ energies of the continuous spectrum. The energy resolution of RNPE spectrum is thus determined by the precision of trigger frequency ω, and not by detected photon energy. This is a key element for successful implementation of the precision neutrino mass spectroscopy, which must resolve photon energies at the μeV level or less, since the (ij) threshold rise at $\omega_{ij}=\epsilon_{eg}/2-(m_i+m_j)^2/(2\epsilon_{eg})$ is separated only a little from the half energy $\epsilon_{eg}/2$ of dangerous PSR.

Calculated rates are sensitive to Majorana CP phases α,β defined by $U_{e2}\propto e^{i\alpha}\,,U_{e3}\propto e^{i\beta}\,.$ Rate rises at $(12),(13),(23)$ thresholds are $\propto(|c_{12}|^2\sin^2\alpha\,,|c_{13}|^2\sin^2\beta\,,|c_{23}|^2\sin^2(\alpha-\beta)\,)$ (the Dirac case given by $|c_{ij}|^2$ without α,β phase), to be further multiplied by an integrated Majorana interference factor of $(1-m_im_j/E_1E_2)$ with E_i neutrino energies. For example, 4 cases of $(\alpha,\beta)=(0,0),(\pi/2,0),(0,\pi/2),(\pi/4,-\pi/4)$ give 3 large threshold phase factors of $(\sin^2\alpha,\sin^2\beta,\sin^2(\alpha-\beta)\,)=(0,0,0),(1,0,1),(0,1,1),(1/2,1/2,1)$ at $(12),(13),(23)$. Since $|c_{12}|^2\approx3\times(|c_{11}|^2,|c_{22}|^2)$ under the given oscillation parameters, the magnitude $\sin^2\alpha$ is most important in rate comparison at low threshold regions, and a small $\sin^2\alpha$ gives a much smaller Majorana rate than the Dirac rate below (33) threshold. We know of no other measurable quantity of this high sensitivity to α and β. Within a given range of neutrino parameters, the easiest observable might be the Majorana phase, as illustrated in our figures. Our proposed experiment is not sensitive to the other CP phase δ, which however may be determined by future neutrino oscillation experiments. Determination of all low energy phases, α,β,δ, is a requisite for a better understanding of leptogenesis [2].

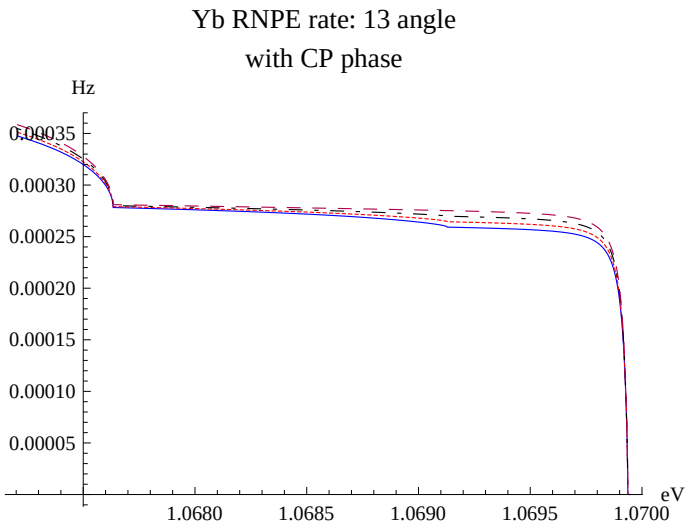

Figure 2: Yb RNPE photon energy spectrum for different $\sin^2\theta_{13}$ values, 0.03 in blue, 0.02 in dotted red, 0.01 in broken black, and 0 in dashed purple, all for $(\alpha, \beta) = (\pi/2, 0)$. Neutrino masses of $(m_3, m_2, m_1) = (50, 10, 5)$meV, and cosine angles $1/\sqrt{2}, \sqrt{3}/2$ for $\cos\theta_{23}, \cos\theta_{12}$ are assumed. Assumed target parameters are $n = 10^{21}\text{cm}^{-3}$, $V = 1\text{cm}^3$, and $\eta = 10^3$.

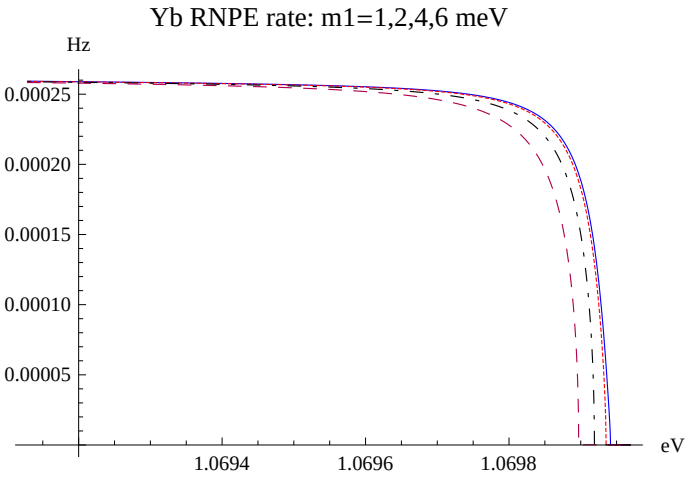

Figure 3: Yb RNPE photon energy spectrum for different m_1 values; 1 meV in blue, 2 meV in dotted red, 4 meV in broken black, and 6 meV in dashed purple, all for $(\alpha, \beta) = (\pi/2, 0)$. Other neutrino masses are constrained by neutrino oscillation experiments, and cosine angles $1/\sqrt{2}, \sqrt{3}/2, \sqrt{0.97}$ for $\cos\theta_{23}, \cos\theta_{12}, \cos\theta_{13}$ are assumed. Assumed target parameters are $n = 10^{21}\text{cm}^{-3}$, $V = 1\text{cm}^3$, and $\eta = 10^3$.

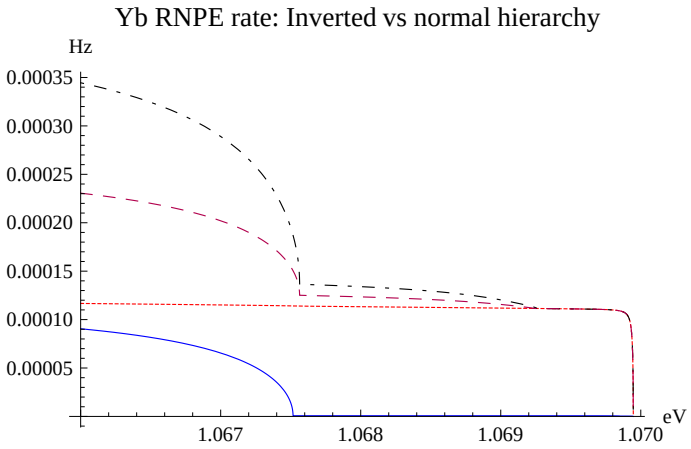

Figure 4: Yb RNPE rate; case of normal and inverted mass hierarchies for different (α, β) values; normal (0,0) (blue), inverted (0,0) (dotted red), inverted $(\pi/2,0)$ (broken black), inverted $(\pi/4, -\pi/4)$ (dashed purple), assuming $m_1 = 5$ meV (other masses constrained by oscillation data) and the same mixing as Fig(3). $n = 10^{21}\text{cm}^{-3}, V = 1\text{cm}^3, \eta = 10^3$.

Distinction of Majorana and Dirac neutrinos is possible by the interference effect of identical Majorana fermions [3], giving different rates in the vicinity of thresholds. Rate difference of Majorana and Dirac pair emission is larger for larger Majorana CP phases, as illustrated in Fig(1). Experimentally, the spectral rate is fitted under an assumption of Majorana or Dirac neutrino and either hypothesis is verified by a good quality of fitting.

One possible serious background against RNPE might be the trigger-less SR due to the achieved excellent coherence. This process has a monochromatic spectrum at $\epsilon_{eg}/2$ different from RNPE, nevertheless it might become dangerous, destroying the initial state. This can be avoided by choosing $J = 0 \to 0$ transition, which forbids single photon emission, complete to any order, hence SR altogether. Alkhali earth atoms have level structure of this angular momentum configuration. Yb and Hg atoms have levels of a similar nature, giving state candidates of $|e\rangle = (6s6p)^3P_0\,, |g\rangle = (6s^2)^1S_0\,, |p\rangle = (6s6p)^1P_1$. Incidentally, two photons emitted by $0 \to 0$ RSR have perfectly correlated polarizations, and may serve as an excellent device of quantum entanglement.

The calculated Yb $0 \to 0$ RNPE rate for $(\alpha, \beta) = (0, 0)$ averaged over all photon energies is $\sim 3 \times 10^{-4}$Hz for $n = 10^{21}\text{cm}^{-3}\,, V = 1\text{cm}^3\,, \eta = 10^3$ (a factor to be better understood) and is by ~ 70 larger than the corresponding Xe $2 \to 0$ rate. When the Yb experiment at each photon energy ω lasts for a day, its event number becomes $O[30]$ if ω is in the energy range of Fig(1). This event number is further increased by f if one repeats condensate formation with a cycle time of $1/f$ sec. We show in Fig(1) and Fig(2) the spectral rate for various combinations of CP phases and the mixing angle θ_{13}. Sensitivity to neutrino masses, in particular to m_1 values, is shown in Fig(3). Determination of m_1 of a few meV range requires a high statistic data near (11) threshold. Distinction of normal (3 neutrino masses given by $m_1, m_2 = \sqrt{0.01^2 + m_1^2}, m_3 = \sqrt{0.05^2 + 0.01^2 + m_1^2}$ eV's) vs inverted (3 masses of $m_1, m_2 = \sqrt{0.05^2 + m_1^2}, m_3 = \sqrt{0.05^2 + 0.01^2 + m_1^2}$ eV's) hierarchies is most dramatic, as seen in Fig(4), hence its determination is easier.

RNPE rate of condensate decay increases like $\propto n^3$, effective with $\alpha_m \propto n$, as the density n increases. The event number from a single soliton decay is smaller than from the condensate decay, typically by $1/(\eta\alpha_m L)$ for a target length $L \gg 1/\alpha_m$ that contains a soliton.

In an ideally coherent medium, field condensate never emits PSR. In practice, there may be a variety of environmental effects that cause a leakage PSR, a potential background to RNPE. One of these effects is a random fluctuation of dielectric constant, most simply due to a density fluctuation $\sqrt{\delta n^2}$. The resulting leakage PSR rate is estimated as

$$\frac{3\mu_{ge}^2\epsilon_{eg}n\sqrt{\delta n^2}V\alpha_m Le^{-(\omega-\epsilon_{eg}/2)^2/\Delta_m^2}}{32\pi\mu}\times\frac{d\omega}{\sqrt{\pi}\Delta_m}\,, \tag{23}$$

for a target length L. We used a Gaussian frequency distribution of width Δ_m for the trigger. We have computed the Yb leakage PSR rate using $\sqrt{\delta n^2}/n$ =5% and Δ_m = 1GHz. The calculated Yb RNPE near (12) threshold of m_1 = 2meV is found much larger than the background PSR. The leakage PSR becomes larger than RNPE, only at photon energies $\leq 2\mu$eV away from the first (11) threshold.

In summary, our proposed method of precision neutrino mass spectroscopy is most sensitive to Majorana/Dirac distinction and to α, β measurements. It is worthwhile to experimentally investigate both formation and long time control of solitons and condensate, which is of crucial importance for controlled detection of PSR and RNPE. Some rudimentary method of efficient soliton formation has been suggested in [6].

Acknowledgements I should like to thank N. Sasao and members of SPAN collaboration for discussion on experimental aspects of this subject, and M. Tanaka for discussion on an aspect of leptogenesis.

This research was partially supported by Grant-in-Aid for Scientific Research on Innovative Areas "Extreme quantum world opened up by atoms" (21104002) from the Ministry of Education, Culture, Sports, Science, and Technology.

References

[1] M. Fukugita and T. Yanagida, *Phys. Lett.* **B 174** 45 (1986).

[2] S. Davidson and A. Ibarra, *Nucl. Phys.* **B648**, 345 (2003), and references therein.

[3] M. Yoshimura, *Phys. Rev.***D75**, 113007(2007).

[4] M. Yoshimura, A. Fukumi, N. Sasao and T. Yamaguchi, *Progr. Theor. Phys.***123**, 523(2010).

[5] M. Yoshimura, C. Ohae, A. Fukumi, K. Nakajima, I. Nakano, H. Nanjo, and N. Sasao, *Macro-coherent two photon and radiative neutrino pair emission*, arXiv 805.1970[hep-ph](2008). M. Yoshimura, *Neutrino Spectroscopy using Atoms (SPAN)*, in Proceedings of 4th NO-VE International Workshop, edited by M. Baldo Ceolin(2008).

[6] M. Yoshimura, *Light Propagation and Paired Superradiance in Coherent Medium*, arXiv:1012.1061 [hep-ph] (2010), and in *Progr. Theor. Phys.***125**,149(2011).

[7] For an excellent review of both the theory and experiments of superradiance, M. Benedict, A.M. Ermolaev, V.A. Malyshev, I.V. Sokolov, and E.D. Trifonov, *Super-radiance: Multiatomic coherent emission*, Informa (1996). For a formal aspect of the theory, M. Gross and S. Haroche, *Phys.Rep.***93**, 301(1982). The original suggestion of superradiance is due to R.H. Dicke, *Phys. Rev.***93**, 99(1954).

[8] L.M. Narducci, W,W. Eidson, P. Furcinitti, and D.C. Eteson, *Phys. Rev.***A 16**, 1665 (1977).

[9] S.L. McCall and E.L. Hahn, *Phys. Rev.***183**, 457(1969). For a review, L. Allen and J.H. Eberly, *Optical Resonance and Two-level Atoms*, Dover, New York, (1975). For comparison with experimental results, R.E. Slusher and H.M. Gibbs, *Phys. Rev.***A4**, 1634(1972).